Experimental study on the aeolian sands solidification via MICP technique

Y.J. Zhou (zyjfcb@126.com)
North China University of Science and Technology https://orcid.org/0000-0001-6498-385X
Hongtao Wang
University of Science and Technology Beijing

Research Article

Keywords: MICP, aeolian sand, solidification, bender element, UCS, SEM

Posted Date: March 22nd, 2021

DOI: https://doi.org/10.21203/rs.3.rs-255149/v1

Abstract

This study solidifies the aeolian sand by microbial induced carbonate precipitation (MICP) technique. The effects of cementation solution with different concentrations, particle size, and grouting batches are examined via the bender element, unconfined compressive test and scanning electron microscope (SEM). The bender element results show that the wave speed of loose aeolian sand is 200m/s; however, after solidify the aeolian sand, the speed of P-wave is about 450-600m/s and S-wave is about 350-500m/s. Additionally, the unconfined compressive strength (UCS) results indicate that when the concentration of cementation solution is 0.75mol/L, the UCS of bio-solidified sand sample is the highest. Then, compared with the aeolian sand with original grade, the particles ranging from 0.1-0.4mm have a better cementation effect. Moreover, the UCS of bio-solidified sand samples increases along with the grouting batch. From the SEM images, it can be seen that when the grouting batch reaches to five times, the particles are almost completely covered by CaCO 3 crystals compared with the three batches and four batches.

Introduction

The mechanism of microbial induced carbonate precipitation (MICP) is that the urease produced by microorganisms and the ammonia gas and carbon dioxide produced by the hydrolysis of urea can be converted into ammonium ion and bicarbonate ion in the alkaline solution environment. Then, the bicarbonate ion will attract calcium ions in solution thus precipitating calcium carbonate. Moreover, as reported, the microorganism is generally negatively charged thereby absorbing positively charged cations such as calcium ions, making the microorganism become the crystal nucleus in the crystallization process of calcium carbonate.

The researchers realized the importance of microbial mineralization as early as 1970s [1, 2]. The researchers in Murdoch University study on the urease activity of bacteria as the research object, and study the effects of nickel ions, grouting methods, and different calcium salt concentrations on the strength of microbial grouting solidified sands [3, 4]. University of Cambridge found that the concentration of nutrients is negatively correlated with the strength of the sample. When the concentration is low, the strength of the sample is higher and the sample integrity is better[5]. Scholars from the University of Glasgow in the United Kingdom have discovered through research that step-by-step grouting can improve the uniformity of calcium carbonate spatial distribution. The calcium carbonate generated in the early and mid-term will help to fix the microorganisms and induce the formation of new calcium carbonate [6]. The research team of King's University in Saudi Arabia discussed the influence of culture medium, bacterial concentration and different buffers on the compressive strength of cement mortar. The strength can reach up to 39.6MPa [7]. Researchers from Monash University found that when the particle size distribution contains 75% coarse aggregate and 25% fine aggregate, the maximum uniaxial compressive strength is about 575kPa. Adding fine aggregate to the coarse aggregate can reduce the size of the coarse aggregate particles. Provide more bridge contact [8, 9]

Lvanov and others applied MICP technology to plugging and improving soil strength in geotechnical engineering [10]. Harkes optimized the MICP grouting technology by the clogging of the grouting port and the unevenness of the sample solidification that often occurred in the experiment [11]. Researchers at the University of California at Davis used microbial solidification to gel the concrete and monitored the shear wave velocity during the repair process [12]. The University of Toronto in Canada successfully reduced the permeability of oilfield sandstone by cementing sandstone particles [13]. Some of the research teams used spraying, immersion and infiltration methods to conduct indoor or on-site microbial coating tests on limestone, marble and sandstone stone samples or actual cultural relics [14-19].

Some scholars have also pay attention to how to improve the economy of the MICP [20]. And Other scholars began to pay attention to adding some other additives to improve the strength of MICP. For instance, Chu Jian of Nanyang Technological University added polyvinyl alcohol fiber and found that the unconfined compressive strength and splitting tensile strength of the sample were increased by 138% and 186% respectively, and the permeability was reduced by 126% [21, 22]. Xu found that the uniaxial compressive performance of the MICP treated sand column has been improved by adding magnesium ions [23]. Cheng tried the surface infiltration method and compared it with the continuous grouting method [24].

Another scholars have studied the MICP by the numerical simulation. The research team of Delft University of Technology in the Netherlands has established a complete mathematical model of the microbial grouting process [25-27].The Swiss Federal Institute of Technology established a model to consider the coupling of various factors, including biology, chemistry, fluids and mechanics[28]. The research team at the University of Northern California used the three-dimensional discrete element method (DEM) to simulate mechanical behavior of silt-stone after MICP reinforcement [29]. ETH Zurich uses CT scanning technology to quantify the key microscopic properties of MICP, such as the size of crystals [30].

The model tests are of great help to MICP research[31-33]. In 2010, scholars from the Delft University of Technology in the Netherlands applied the technology of microbial induction to generate calcium carbonate in the on-site sandy gravel soil reinforcement project [34, 35]. Van Passen used microbiological methods to carry out $1m^3$ and $100m^3$ sand samples for prototype sand foundation reinforcement tests [36].

In summary, some research results have been made in the MICP technique for solidifying various saturated sand and unsaturated sand. Including metallogenic mechanism of sand, grouting reinforcement method and nutrient concentration for the effect of mineralization. However, the aeolian sand is different from the solidifying various saturated sand as well as unsaturated sand, because of the much lower moisture content and the much poorer particles size distribution. Meanwhile there is no effect on solidifying aeolian sand by using the traditional foundation reinforcement methods. In addition, there is few research on the MICP for aeolian sand solidification. Therefore, it is very necessary to carry out research on aeolian sand solidification via MICP.

Materials And Methods

Materials

Aeolian sand selection

The aeolian sand used in the current study was sampled (0.3m below the ground surface) from the Kubuqi Desert, China (Latitude: 40.46212, Longitude: 108.653344), which is the ninth largest desert in the world and the sixth largest in China (Figure 1). Due to physical weathering and chemical weathering, the aeolian sand particles are angular, weak in strength, uneven in size distribution, and contain a certain amount of fine soil particles.

Physical properties of aeolian sand

Natural moisture content calculation

According to GB/T50123-1999

geotechnical test standards of China, the natural moisture content test needs to be carried out twice and its arithmetic average is taken. The formula of natural moisture content for aeolian sand is followed:

$$Wo=(m0/md-1)\times100\% \quad (1)$$

m0 is the quality of wet soil (g), and md is the quality of dry soil (g). The testing results of natural moisture content of aeolian sand are shown in Table 1. The natural moisture content of aeolian sand is about 0.80% by calculating.

Table 1 Test on natural moisture content of aeolian sand

Number	Quality of wet sands/g	Quality of dry sands/g	Quality of water/g	Moisture content /%	Average of moisture content /%
1	15.98	15.85	0.13	0.82	0.8
2	19.31	19.16	0.15	0.78	

Particles size distribution analysis

The particle size distribution is presented in Figure 2. As can be seen, the particles size distribution of the aeolian sand is mainly between 0.1mm and 0.4mm.

Table2 Aeolian sand particle size distribution

size（mm）	<0.075	<0.1	<0.2	<0.3	<0.4	<0.5	<0.6	<0.7	<1
percentage（%）	0.055	2.807	64.583	87.067	98.542	99.733	99.768	100	100

According to the figure 2, the particles size distribution of the aeolian sand is mainly between 0.1mm and 0.4mm. Additionally, the effective particle is d_{10}=0.11, the Median is d_{50}=0.17, the limit particle size is d_{60}=0.19 and d_{30}=0.14. The uneven coefficient of aeolian sand is $Cu=d_{60}/d_{10}$=1.73; and the curvature coefficient is $C_C=d_{30}^2/(d_{60}\times d_{10})$=0.74.

pH measurement

According to GB/T50123-1999

geotechnical test standards of China, the pH value of suspension water of aeolian sand is 8.77.

Bacteira

The microbial used in the current study is sporosarcina pasteuri, which has a strong survivability as well as a high urease production ability. The cell surface is negatively charged, the spores are oval or spherical, the cell rod is 2-3μm long and 1-2μm in diameter. The process of bacterial culture is presented in figure 4. The average urease activity is about 15.01mmol/min, and the average OD600=2.62.

Fixation and cementation solution

The cementation solution herein is composed of $CaCl_2$ and urea, which is analytically pure and were provided by Shanghai Titan Reagent Co., Ltd. In this study, the detailed experimental scheme is shown in Table 3.

Methods

Sample preparation

For each sample, 115g dry sand particles were packed into a column. The grouting and solidification process of aeolian sand is carried out in a medical syringe. Other instruments mainly include: balance, geo-nonwoven fabric, labeled sand, funnel, beaker, purified water, tray, retainer, peristaltic pump and so on. Studying the effects of different concentrations of CaCl2, particles size distribution and different grouting batches respectively.

Table 3 Experimental scheme

Fixation solution	Concentration of fixation solution/mmol/L	Cementation Solution	Concentration of Cementation solution /mol/L	Particles size distribution	Grouting batches
$CaCl_2$	25	$CaCl_2$+CH_4N_2O	0.25	Particles all size/	3 times
	50		0.5		**4 times**
	75		**0.75**	Particles size in**0.1-0.4mm**	5 times
	100		1.0		
	150		1.5		

Note: The black font in table 3 represents the basic plan.

Particles size distribution

It is selected the particles all-size distribution and particles size from 0.1mm to 0.4mm under the premise of the basic scheme. As can be seen from figure 2, the range from 0.1mm to 0.4mm of particles size are more particles in test. The particles size range that is too large (>0.4mm) and too small (<0.1mm) are removed.

Grouting batches

It is selected different grouting batches including three times, four times and five times to research, and the grouting process is shown in figure 3(d). After the grouting and solidification is completed, the syringe is divided into two parts with a tool, from which the aeolian sand column is taken out and labeled. As the shown in figure3(f).

Results

Bender element test

The test uses the bender element BES in conjunction with the data acquisition system. It is selected two size of probes to measure the wave speeds for loose aeolian sand and solidified aeolian sand column respectively, and the loose aeolian sand is to be contrast one. The bender element shown in figure 4.

The electromagnetic wave propagates through the piezoelectric ceramic plates at the ends of two probes of the bender element , ones is the transmitting wave device and the other one is the receiving wave device, completing a test cycle. It is evaluated the degree of different solidification aeolian sand through measuring the speed of P-wave and S-wave. The process of measuring is shown in figure 5 and some part of curves for waves are shown in figure 6.

As can be seen from the figure 7, neither P-wave nor S-wave continuously increases with the increase of nutrient concentration, but there is a peak value. When the concentration is 0.75mol/L, the solidification of aeolian sand is more better than others concentration by using the MICP. The value for speed of P-wave is bigger than the S-wave from the figure11, and the speed of P-wave is more 1.3 times than the speed of S-wave from the figure 8 fitting results.

As can be seen in the figure 9 and figure 10, the wave speed of the particles all-size distribution is smaller than that of the particles size from 0.1mm to 0.4mm. The comparative test shows that the particles size are controlled in a relatively uniform range, which can make the pores between particles larger. The $CaCO_3$ is much easier to cement, and the degree of cementation is much more better.

There are three different kinds of nutrient concentrations to research, including 0.5mol/L, 0.75mol/L and 1mol/L. It can be seen from figure 11 that under the same nutrient concentration, the largest wave speed of the grouting batches is the five batches, the maximum are the 470m/s, 550m/s and 500m/s respectively. It shows that grouting batches are beneficial to improve the solidification aeolian sand. Among the three different nutrient concentrations, the 0.75mol/L has a relatively large S-wave speed, which is roughly distributed in the range of 450-550m/s and the average value is higher than the other two concentrations. It also shows that when nutrient concentration is 0.75mol/L, the aeolian sand solidification is much better.

Unconfined compressive strength (UCS)

The dried bio-cemented aeolian sand samples are cut into two parts (A and B), then their surfaces are ground flat with a grinding machine to eliminate the influence of deviant stress in the compression process (figure 12 and figure 13). The testing machine is MTS810, and the loading rate is 1mm/min, controlled by the displacement. It records the process from loading to specimen failure, and the peak stress is the unconfined compressive strength of the specimen. Representative stress-strain curves as presented in figure 14.

The UCS results are drawn in Figure 15. It can be seen that the UCS of bio-cemented aeolian sand samples increases when the concentration of cementation solution increases from 0.5mol/L to 0.75mol/L. However, when the concentration becomes larger than 0.75mol/L, then UCS decrease. Additionally, the average value of UCS for the aeolian sand column increase along with the number of injections.

Scanning electron microscope (SEM)

The SEM images concerning crystal polymorph and microstructures of bio-cemented sand samples are shown in figure 16 and 17. Compared with the loose sand particles presented in figure 1, the aeolian sand particles after MICP treatment are covered by $CaCO_3$ crystals. . It is found that the morphology of precipitated $CaCO_3$ crystals is mostly cubic as shown in figure 16(a) and16(d). From figure 16(b)-(c)-(e)-(f), there are some round or slender rod-shaped holes showing on the $CaCO_3$ surfaces which are identified

as the bacterial traces. The diameter of round holes is about 1micron, while the rod-shaped holes are 3-4 microns in length.

It is the precipitated $CaCO_3$ crystals acting as the cementitious materials which bond the loose sad particles together thus improving the mechanical properties of sand. With the increase of the grouting times, the living environment of microorganisms in the reaction system will be changed, which is conducive to the attachment of microorganisms on the surface and joints of sand particles to form crystalline nuclei. It is also conducive to produce the $CaCO_3$ for increasing the sand strength.

As shown in figure 17, compared with four batches grouting, the amount of $CaCO_3$ crystals precipitated by five batches injection with same cementation solution concentration are much higher. As for the different concentration, 0.75mol/L can induced more CaCO3 crystals than other concentrations, which corresponding to figure 17 where the 0.75mol/L can induce the highest UCS (26.09MPa).

Conclusion

Based on the experimental results, the following conclusions can be drawn:

(1) Compared with the loose aeolian sand where the wave speed is only 200 m/s, the P-wave speed of bio-cemented aeolian sand column is about 450-600m/s and S-wave speed of it is about 350-500m/s by the bender element test. It has been improved obviously, compared with loose aeolian sand with a wave speed of 200m/s.

(2) This study investigated the effects of different concentrations of cementation solution. When the concentration of cementation solution is 0.75mol/L, the speeds of P-wave and S-wave and the unconfined compression strength of bio-cemented aeolian sand are highest.

(3) The best times of batches is five times and the best nutrient concentration is 0.75mol/L. The average of uniaxial compressive strength is 26.4MPa under this condition. It is higher than that of four batches (16.51MPa) and three batches (13.77MPa). The results show that the solidification effect of aeolian sand is more much better base on microbial induced carbonate precipitation (MICP).

Declarations

All the authors declare that there is ethical approval, the data and materials is available.

Everybody consents to participate and to publish.

Contribution Zhou: Conceptualization, Methodology, Investigation, Formal analysis, Writing - original draft.

Wang: Supervision, Validation, Funding acquisition, Writing - review & editing.

Funding Information This study is supported by Hebei Provincial Universities' Basic Scientific Research Operating Expenses (No.JQN2020027), the doctoral Research Initiation Fund of North China University of Science and Technology (No.28418599).

Conflicts of Interest The authors declare that they have no conflicts of interest.

References

1. Kaltwasser, H.K.J. (1972). Control of Urease Formation in Certain Aerobic Bacteria.Arch. *Microbiol*, 81, 178-196.
2. Stocks-fischer, S., Galinat, J.K., Bang, S. (1999). Microbiological precipitation of $CaCO_3$. *Soil Biology& Biochemistry*, 31, 1563-1571.
3. Van, P.L. (2009). Biogrout, ground improvement by microbial induced carbonate precipitation. *Delft University of Technology.*
4. Salwa,(2008). High strength in-situ biocementation of soil by calcite precipitating locally isolated ureolytic bacteria. *Murdoch University.*
5. Cheng, L., Cord-ruwisch, R., and Shahin, M. (2013). Cementation of sand soil by microbially induced calcite precipitation at various degrees of saturation. *Canadian Geotechnical Journal*, 50, 81-90.
6. Al, Q.A., Soga,, (2013). Effect of chemical treatment used in MICP on engineering properties of cemented soils. *Geotechnique*, 63, 331-339.
7. Tobler, D.J., Maclachlan, E. (2012). Phoenix V R. Microbially mediated plugging of porous media and the impact of differing injection strategies. *Ecological Engineering*, 42, 270-278.
8. Al-salloum, Y., Abbas, H., and Sheikh, Q.I. (2017). Effect of some biotic factors on microbially-induced calcite precipitation in cement mortar. *Saudi journal of biological sciences*, 24, 286-294.
9. Mahawish, A., Bouazza, A., and Gates, W. (2018). Effect of particle size distribution on the biocementation of coarse aggregates. *Acta geotechnic*, 13,1019-1025.
10. Ivanov, V., Chu, (2008). Applications of Microorganisms to Geotechnical Engineering for Bioclogging and Biocementation of Soil in Situ. *Reviews in Environmental Science and Biotechnology*, 7, 139-153.
11. Harkes, M.P., Van, P.L.A, Booster, J.L. (2010). Fixation and Distribution of Bacterial Activity in Sand to Induce Carbonate Precipitation for Ground Reinforcement. *Ecological Engineering*, 36, 112-117.
12. Dejong, J.T. (2006). Fritzges M B, Nusslein K. Microbially induced cementation to control sand esponse to undrained shear. *Journal of geotechnical and geoenvironmental engineering* ,132, 1381-1392.
13. Ferris, F., Stehmeier, L., and Kantzas, A. (1997). Bacteriogenic mineral pluggin]. *Journal of Canadian Petroleum Technology*,
14. Achal,V.,Pan, X., and Fu,(2011). Biomineralization based remediation of As(III) contaminated soil by Sporosarcina ginsengisol. *Journal of Hazardous Material*s, 201-202,178-184.

15. Achal, V., Mukherjee, A., Reddy, M.(2010). Microbial concrete: way to enhance the durability of building structures. *Journal of Materials in Civil Engineering*, 23, 730-734.
16. Le, M.G., Castanier, S. and Orial, (1999). Applications of bacterial of limestones in buildings and historic patrimony the protection and regeneration. *Sedimentary geology*, 126, 25-34.
17. Rodriguez-navarro, C., Rodriguez-gallego, M., and Chekroun,K.(2003). Conservation of ornamental stone by Myxococcus xanthus-induced carbonate biomineralization. *Applied and Environmental Microbiology*, 69,2182-2193.
18. Muynck, W. Leuridan, S. and Loo, D.V.(2011). Influence of pore structure on the effectiveness of a biogenic carbonate surface treatment for limestone conservation. *Applied Environmenta Microbiology*, 77, 6808- 6820.
19. Zamarreno, D.V., Inkpen, R.M. and May, (2009). Carbonate crystals precipitated by freshwater bacteria and their use as a limestone consolidant. *Applied & Environmental Microbiology*, 75, 5981-5990.
20. Rowshanbakht, K., Khamehchiyan, M., and Sajedi, R.(2016). Effect of injected bacterial suspension volume and relative density on carbonate precipitation resulting from microbial treatment. *Ecological engineering*, 89,49-55.
21. Dhami, N.K., Reddy, M.S. and Mukheriee, (2016). Significant indicators for biomineralisation in sand of varying grain sizes. *Construction and building materials*, 104, 198-207.
22. Choi, S., Wang, K. and Chu, (2016). Properties of biocemented, fiber reinforced sand. *Construction and building materials*, 120,623-629.
23. Xu,C., Guo, H.X. and Cheng, X.H. (2020). The promotion of magnesium ions on aragonite precipitation in MICP process. *Construction and Building Materials*, 263.
24. Cheng, L., Cord-Ruwisch, (2012). In Situ Soil Cementation with Ureolytic Bacteria By Surface Percolation. *Ecological Engincering*, 42, 64-72.
25. Van,W.W.K,Vermolen, F.J. and Van, M.G.A.(2011). Modelling Biogrout: A New Ground Improvement Method Based on Microbial-induced Carbonate Precipitation. *Transport in Porous Media*, 87, 397-420.
26. Van, W.W. K., Vermolen, F.J. and Van, M.G.A.M. (2012). Mathematical Model and Analytical Solution for the Fixation of Bacteria in Biogrout. *Transport in Porous Media*, 92, 847-866.
27. Van, W.W. K., Vermolen, F.J. and Van, M.G.A.M. (2013). A mathematical model for Biogrout. *Computational Geosciences*, 17, 463-478.
28. Fauriel,S.,Laloui,(2012). Abio-chemo-hydro-mechanical model for microbially induced calcite precipitation in soil. *Computers and Geotechnics*, 46,104-120.
29. Terzis, D., Laloui, (2018). 3-D micro-architecture and mechanical response of soil cemented via microbial-induced calcite precipitation. *Scientific reports*, 8, 1416.
30. Cheng, X.H., Yang, Z., and Zhang, Z. (2013). Modeling of Microbial Induced Carbonate Precipitation in Porous Media. *Joumal of Pure and Applied Microbiology*, 7, 449-458.

31. Li, (2014) Geotechnical properties of biocement treated soils. *Nanyang Technological University*.
32. Whiffin, V.S., Van, P.L.A. and Harkes, M. (2007). Microbial carbonate precipitation as a soil improvement technique. *Geomicrobiology Journal*, 24, 417- 423.
33. Martinez, B.(2012). Upscaling of Microbial Induced Calcite Precipitation in Sands for Geotechnical Ground Improvement. *Dissertations & Theses -Gradworks*,2012.
34. Van,P.L.(2011).Bio-mediatedground improvement: from laboratory experiment to pilot applications. *Geo-Frontiers: Advances in Geotechnical Engineering*. Dallas: ASCE, 4099-4108.
35. Van, D.S.W.R.L., Van, W.W. K.L.A. (2011). Stabilization of gravel deposits using microorganisms. *Proceedings of the 15th European Conference on Soil Mechanics and Geotechnical Engineering*. Athens: IOS Press, 285-90.
36. Van, P.L.A., Harkes, M.P. and Van, Z.A. (2009). Scale up of Biogrout: A biological ground reinforcement method. Proceedings of the 17th International Conference on Soil Mechanics and Geotechnical Engineering. [S.l.]: Lansdale IOS Press, 2328-2333.

Figures

Figure 1

The location of Kubuqi Desert, and SEM image for aeolian sand particles. Note: The designations employed and the presentation of the material on this map do not imply the expression of any opinion whatsoever on the part of Research Square concerning the legal status of any country, territory, city or area or of its authorities, or concerning the delimitation of its frontiers or boundaries. This map has been provided by the authors.

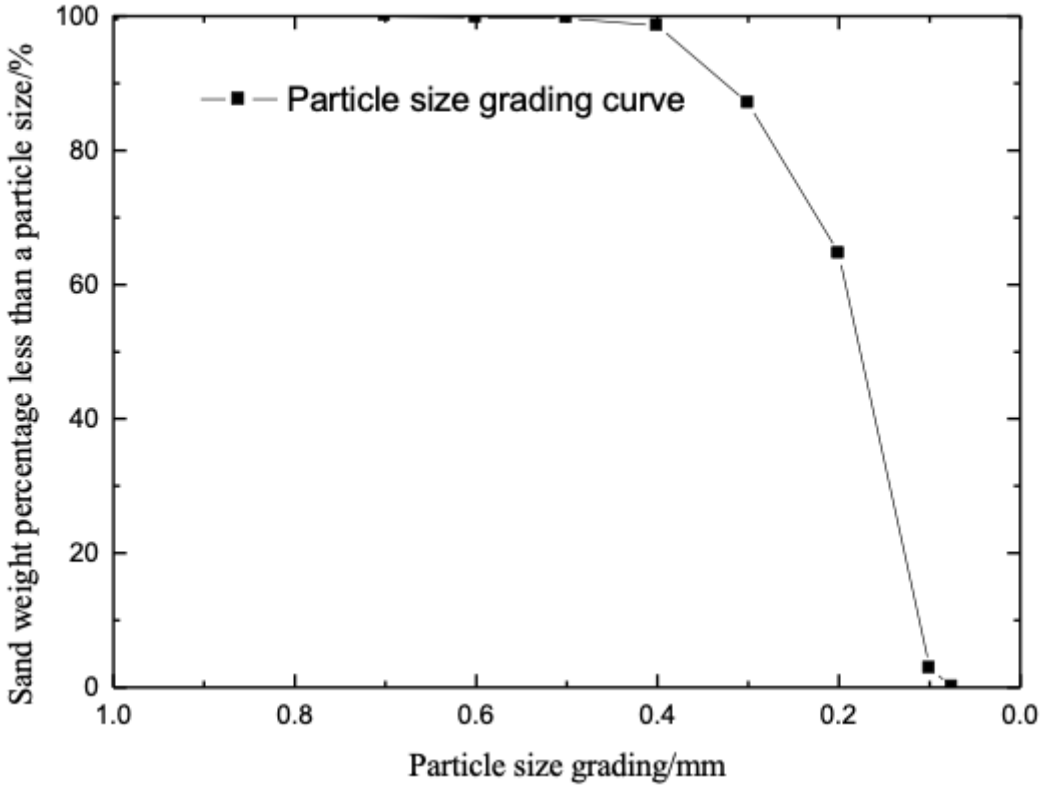

Figure 2

Particle size distribution of aeolian sand

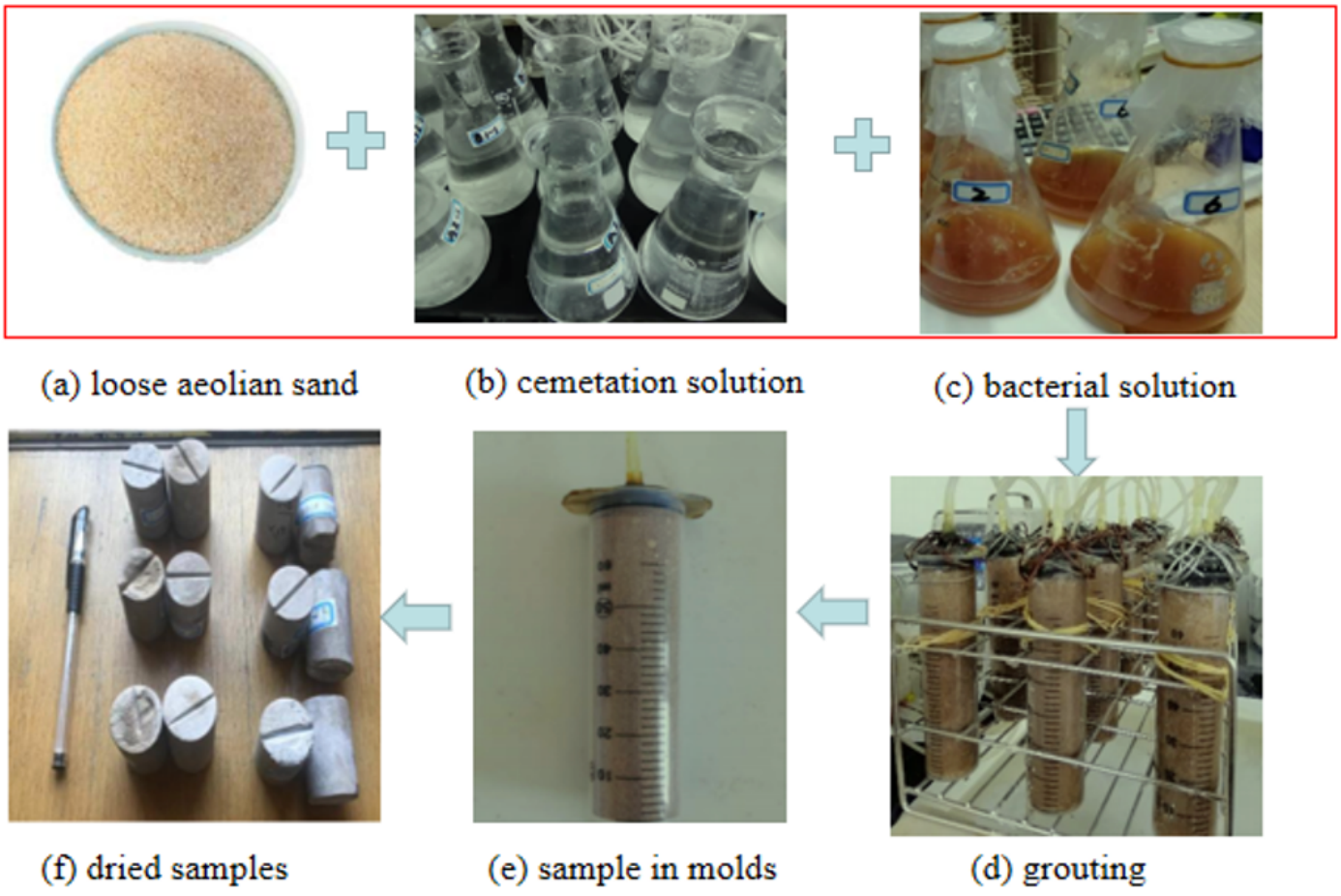

Figure 3

The process of microbial grown

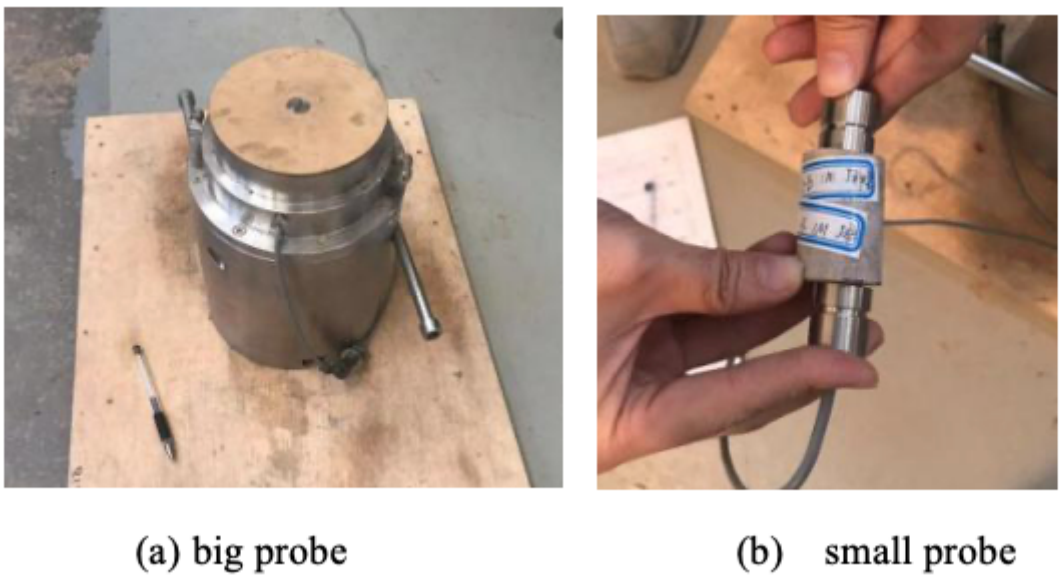

Figure 4

Bender element

(a)Measuring the loose sand (b)Measuring the solidified sand

Figure 5

The process of testing the bender element

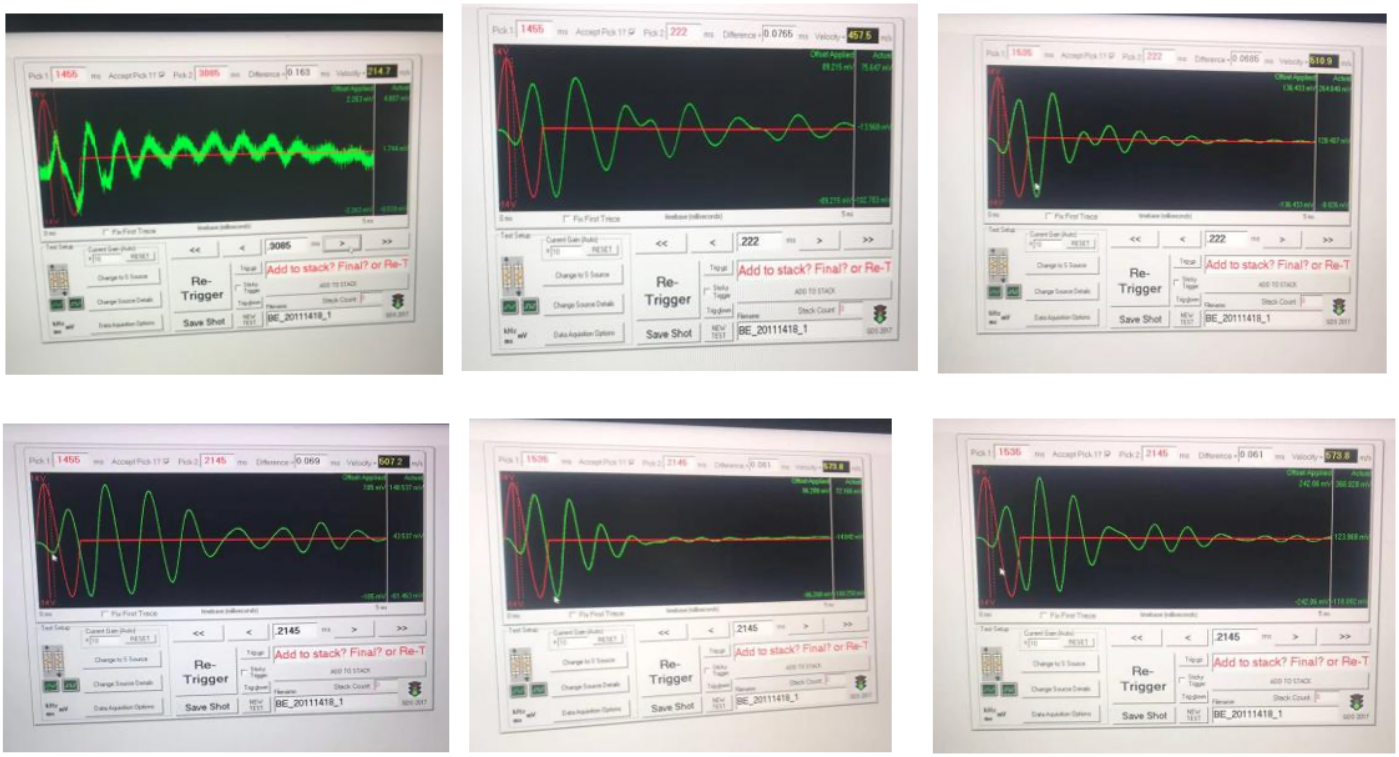

Figure 6

Part of the testing sand wave

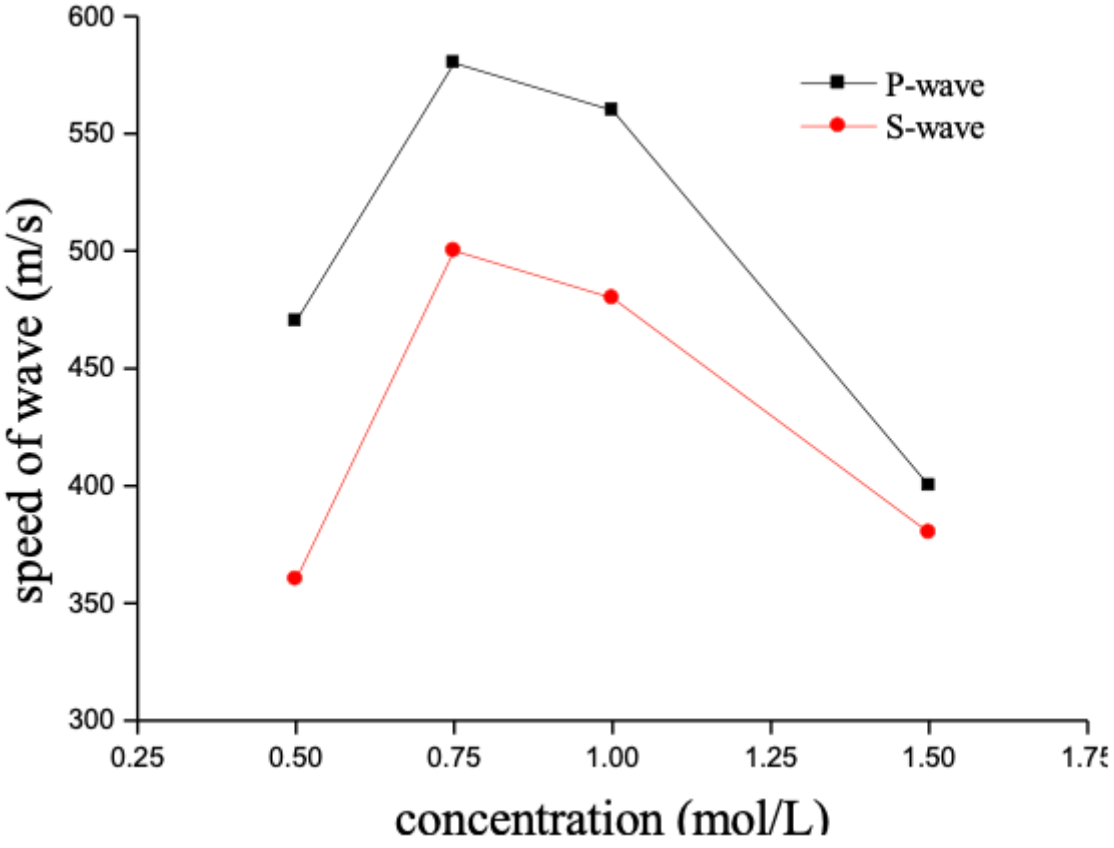

Figure 7

The wave speed of different nutrient concentration

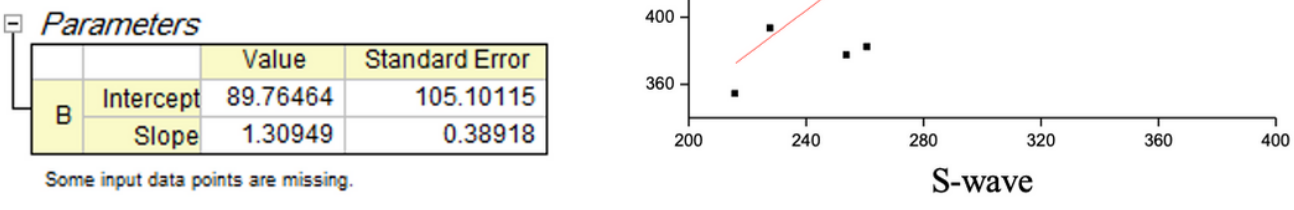

Parameters

		Value	Standard Error
B	Intercept	89.76464	105.10115
	Slope	1.30949	0.38918

Some input data points are missing.

Figure 8

Curve fitting of P-S wave

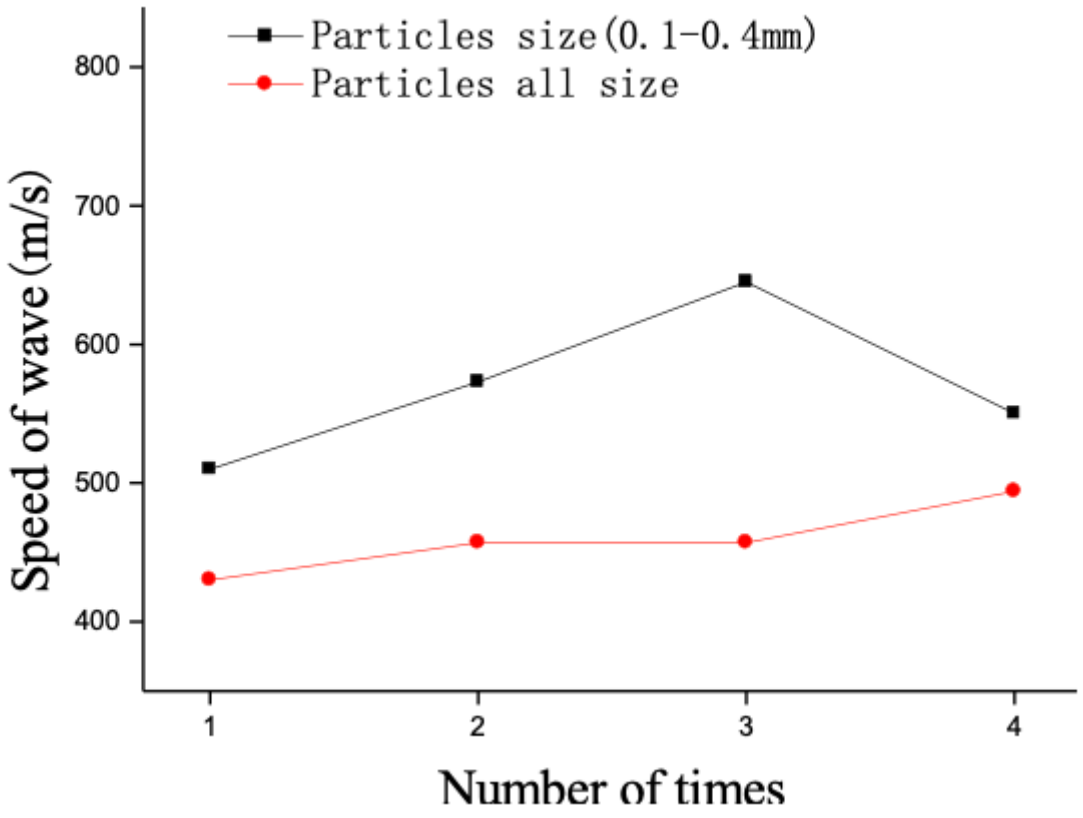

Figure 9

The wave speed for 1mol/L

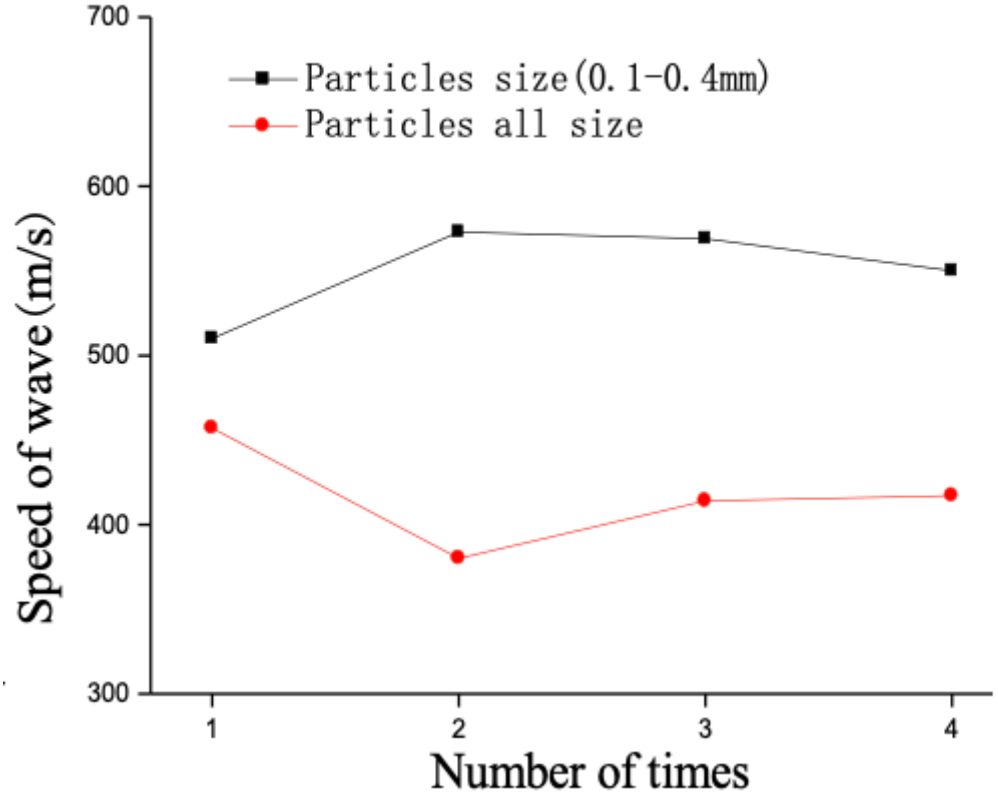

Figure 10

The wave speed for 1.5mol/L

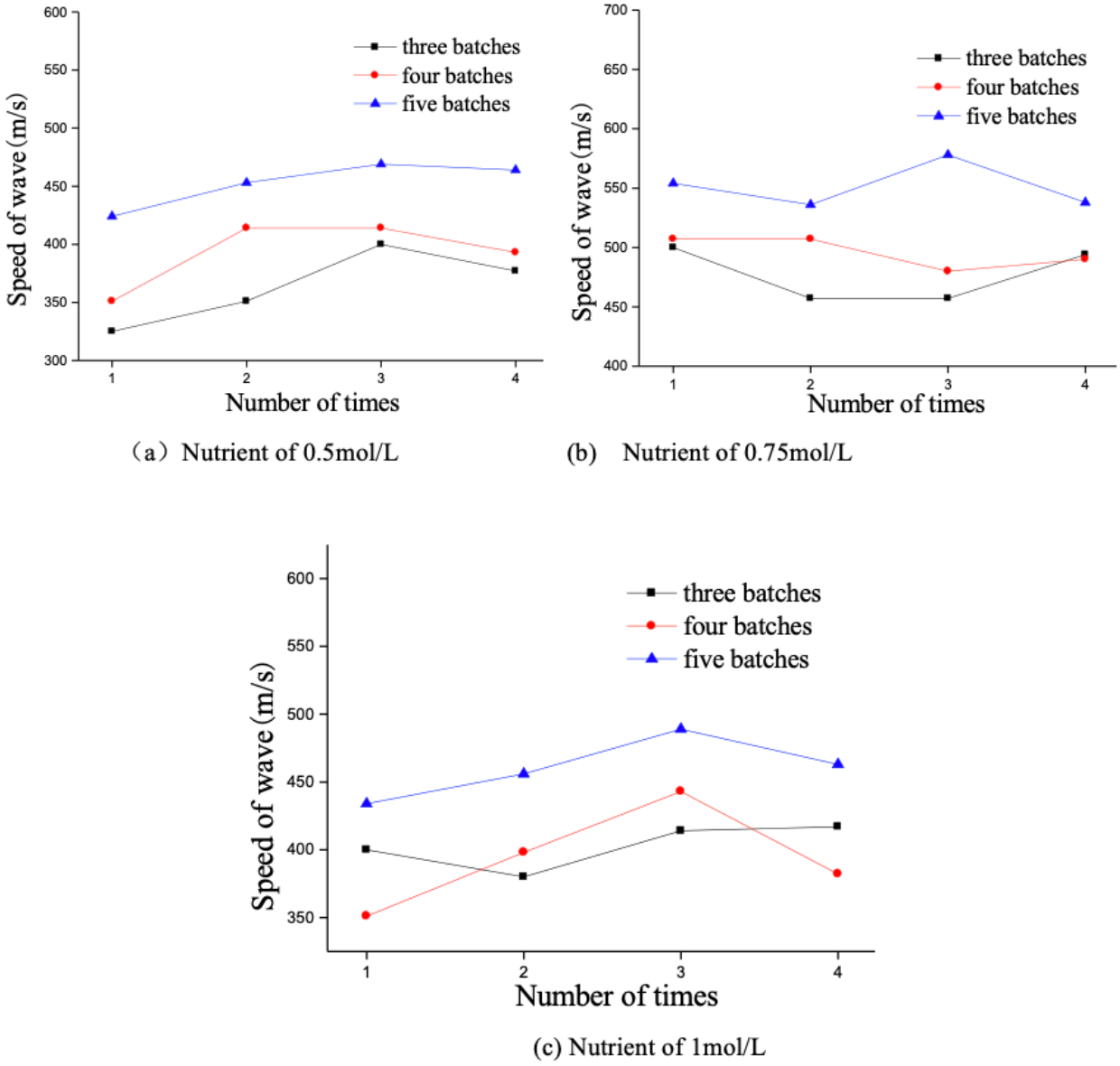

Figure 11

Comparison chart of wave speed for different grouting batches

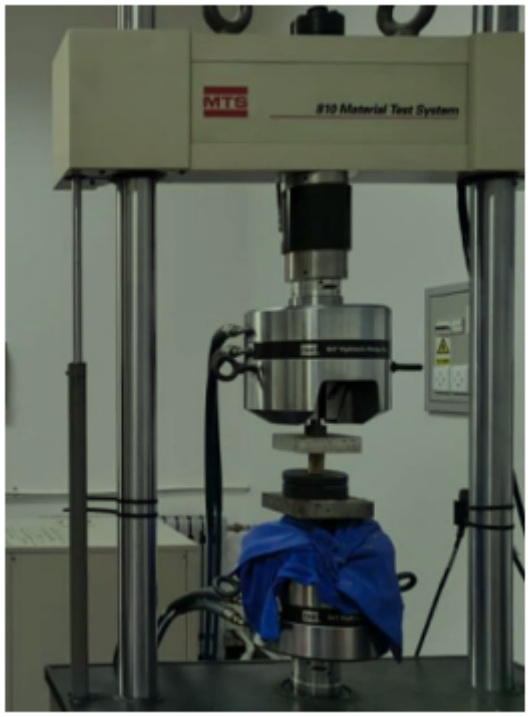

Figure 12

Test machine

Figure 13

Specimen failure under loading

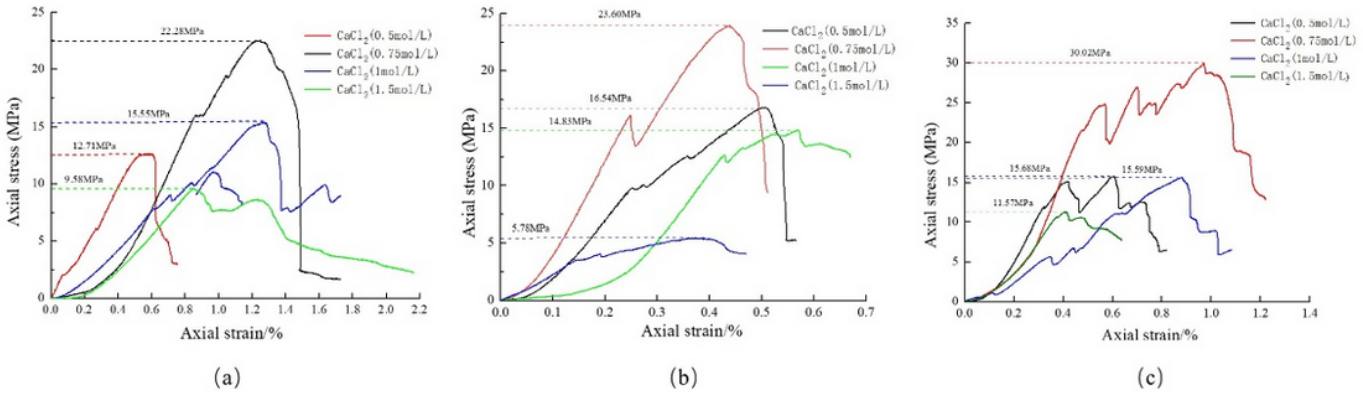

Figure 14

The respresentive stress-strain curves for UCS (a) three batches grouting, (b) four batches grouting, and (c) five batches grouting

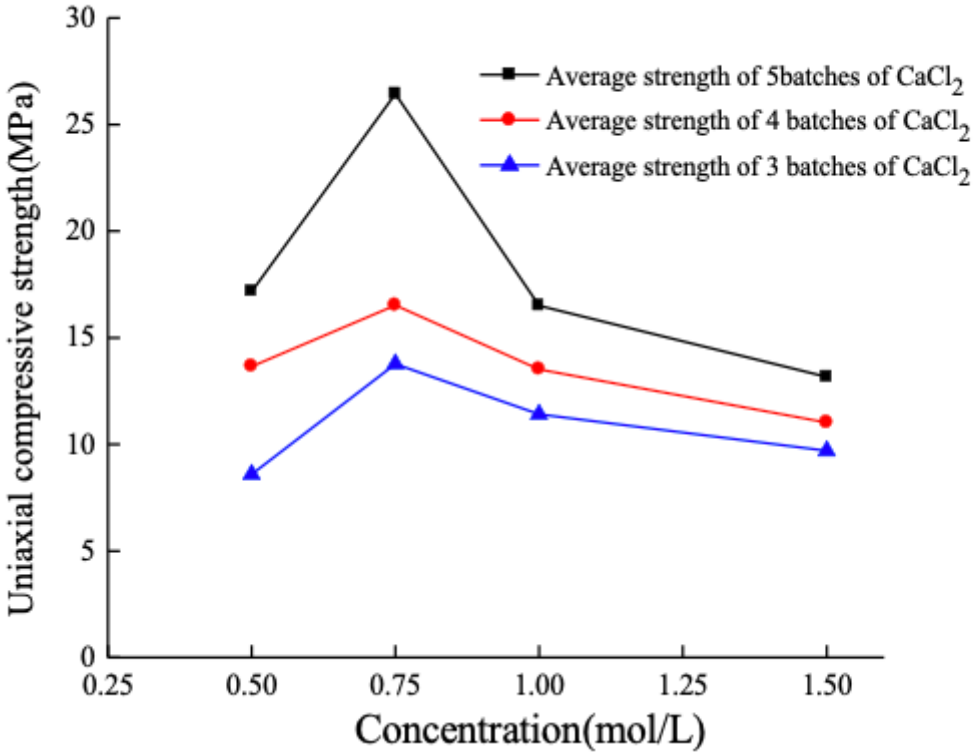

Figure 15

The uniaxial compressive strength in different batches

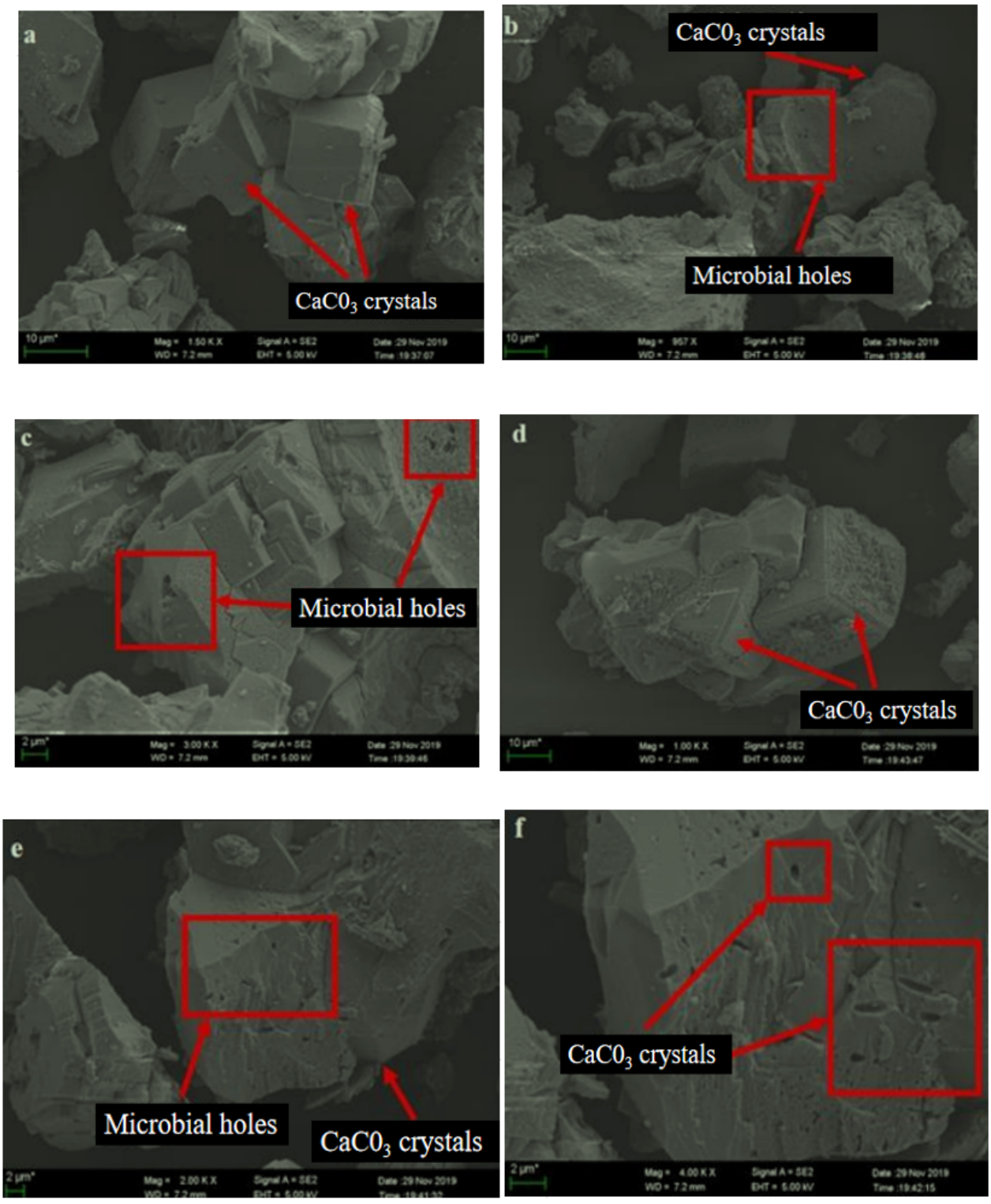

Figure 16

Cementitious materials generated by MICP

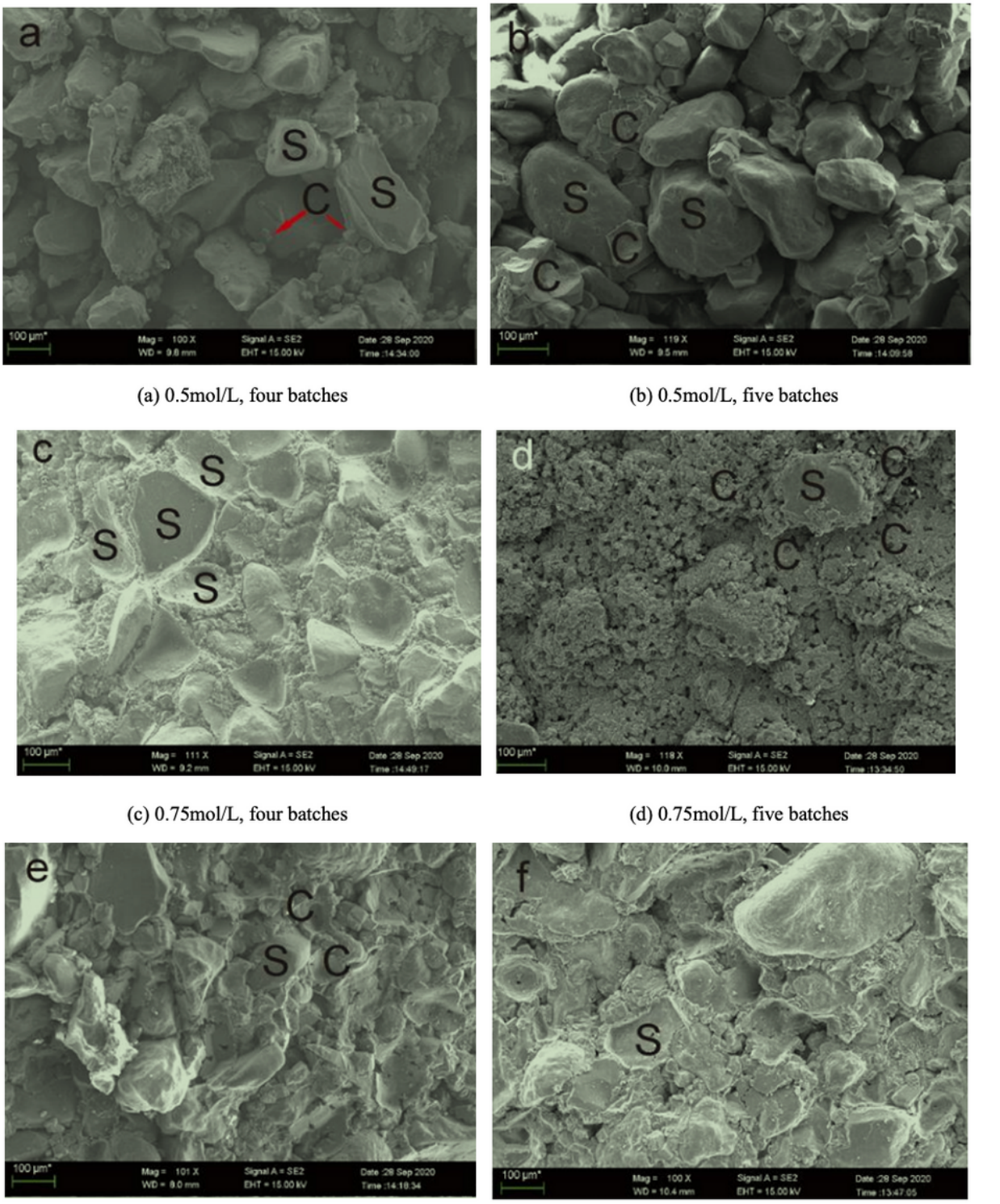

Figure 17

The production of CaCO3 at different concentration and different batches